

# Compact Ultra-Wideband Multilayer Patch Antenna with Defected Ground Plane for Ku Band Applications

Kiran N. Patil, Mownika T. Raj, Chethana K. A., Ajay K. Dwivedi,  
Nagesh K. Narayanaswamy, Vivek Singh

**Abstract –** A circular ring-loaded compact ultra-wideband microstrip patch antenna with a defected ground plane is introduced in this work. The proposed antenna has a multilayer (three layers) configuration consisting of two substrates (FR-4 epoxy with relative permittivity of 4.4 and Air with relative permittivity of 1) as a dielectric medium. When it comes to antenna specifications for Ku/K band applications, the proposed antenna is compared and surveyed against previously reported antennas. Stacking and the defective ground plane are used to enhance the impedance bandwidth. Optimization is also performed in terms of the dimension of the slot made on the lower patch and the number of circular rings made on the upper patch to obtain the optimized ultra-wideband antenna structure. The operating frequency range of the proposed antenna is 12.4 GHz to 18.6 GHz; thus, the antenna applies to Ku band applications. Antenna performance is discussed in terms of  $|S_{11}|$ (dB), gain and radiation efficiency.

**Keywords** –Ultra wideband, Multilayer, Surface Current, HFSS, Ringing effect, Ku band.

## I. INTRODUCTION

Recent developments in the micro-electromechanical system (MEMS), monolithic microwave integrated circuits (MMICs), and Hybrid MMICs increase the demand for miniaturization of associated electronics components and devices in communication system modules. In the process of miniaturization of a wireless communication system module, one of the basic key elements and constraints is antenna size. Microstrip patch antennas have a great demand over other antennas in leading wireless communication technologies because of their ease of integration with other monolithic microwave integrated circuits (MMICs), compactness, low profile configuration, and low cost [1]. A microstrip antenna's low gain and narrow bandwidth severely restrict its usefulness. To satisfy the need for high impedance bandwidth, performance must be improved. A tremendous amount of work is carried out by various researchers and scientists to overcome these shortcomings. Many techniques have been recommended to obtain large impedance bandwidth

*Article history:* Received November 11, 2022; Accepted March 10, 2023

Kiran N. Patil, Mownika T. Raj, Chethana K. A., Ajay K. Dwivedi, Nagesh K. Narayanaswamy and Vivek Singh are with the Department of Electronics and Communication Engineering, Nagarjuna College of Engineering and Technology, Bengaluru, Karnataka, India, E-mail: kirannpatil18@gmail.com, mownikatraj@gmail.com, chethanaka10@gmail.com, er.ajaydwivedi@gmail.com, nageshlakmaya@gmail.com, vivek.10singh@gmail.com.

(wideband/ultra-wideband (UWB)) and gain, such as stacking of patch antenna [2, 3], providing slot and notch on the patch [3, 4] use of planar monopole antennas and defected ground structure [5]-[10]. The demand and necessity for the ultra-wideband (UWB) patch antennas are continuously increasing since the federal communication commission (FCC) defined an unlicensed frequency band range of 3.1 GHz to 10.6 GHz in 2002 for different commercial wireless applications [11]. In UWB technology, a single patch antenna replaces various narrowband patch antennas, which may effectively reduce fabrication and manufacturing costs. Researchers and scientists have documented a variety of patch antenna designs for use in ultra-wideband (UWB) applications ranging from 3.1 GHz to 10.6 GHz ever since the invention of the patch antenna [12]-[17].

In the last few years, the focus of the researchers is moving toward the modelling and simulation of patch antennas in the higher frequency range because of congestion and saturation of work in the lower frequency range (< 10 GHz). However, researchers are still working to obtain the UWB patch antennas for higher frequency range (> 10 GHz) with compact configuration and optimum characteristics. To carry on this inquiry, multiple patch antenna layouts are offered by different researchers for Ku/K band applications. [18]-[27]. Microstrip patch antennas operating in the range of 12-20 GHz (Ku band) are listed in Table I and a comparative analysis is performed between the reported antennas and the proposed antenna.

In Table 1 the comparative analysis is carried out in terms of the size of the antenna structure, substrate materials, impedance bandwidth, peak gain, and radiation efficiency. Antennas mentioned in [18]-[22] have single resonating bands, antennas reported in [23]-[25], [27] have dual resonating bands, and the antenna reported in [26] has triple resonating bands for Ku/K band applications. Table 1 shows that the proposed antenna has a smaller patch area (in mm<sup>2</sup>) than the antennas described in [20, 22, 24, and 27] by a factor of 2.4, 2.25, 3.5, and 1.02 respectively, and greater than the antennas reported in [18, 19, 21, 25, 26] by a factor of 1.42, 1.42, 1.7, 5.6 and 1.33 respectively. The patch area of the antenna reported in [23] is equal to the patch area of the proposed antenna. However, the impedance bandwidth (12.4-18.6 GHz - 40.8%) of the proposed patch antenna is greater than the impedance bandwidth of all other reported antennas in Table 1.

It can be seen from a comparison of the peak gain (dB) of the proposed antenna and the reported antenna that the

proposed patch antenna has a somewhat lower peak gain than the antennas published in [19]-[21] whereas sufficiently larger than the antennas reported in [18], [22]-[27]. The radiation efficiency of the proposed patch antenna (88.40 %) is greater than the radiation efficiency of the antennas reported in the table except for the antenna reported in [19].

TABLE 1

COMPARATIVE INVESTIGATION IN TERMS OF CRITICAL PARAMETERS BETWEEN THE SUGGESTED ANTENNA AND PREVIOUSLY REPORTED ANTENNA

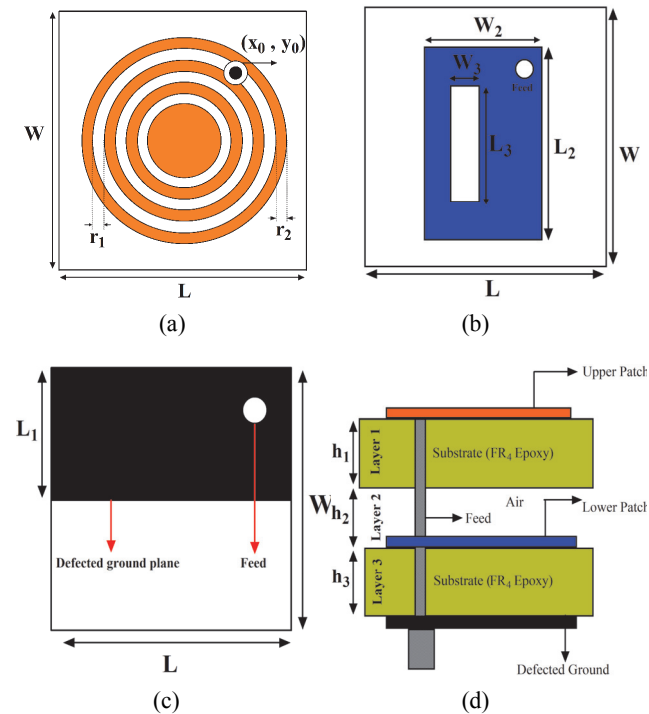
Ref.	Antenna area size (mm <sup>2</sup> ) & (Substrate)	Bandwidth (in GHz)/(%IBW)/ (Bandwidth frequency range GHz)	(Peak gain in dB)/ Radiation efficiency in %
[18]	20×14=280 (FR4 Epoxy, $\epsilon_r = 4.6$ )	4.3/(24.76) / (15.35–19.65)	(6.2)/88.2
[19]	20×14=280 (FR4 Epoxy, $\epsilon_r = 4.6$ )	1.38/(7.74) / (17.15–18.53)	(7.8)/89.97
[20]	80×12=960 (Taconic, $\epsilon_r = 2.25$ )	1.62/(11.45) / (13.36–14.98)	(7.8)/NR
[21]	15×15=225 (RT/Duroid 5880, $\epsilon_r = 2.2$ )	0.95/(7.77) / (11.76–12.71)	(7.6)/NR
[22]	30×30=900 (Glass, PTFE, $\epsilon_r = 2.5$ )	2/(13.36) / (14–16)	(6.3)/NR
[23]	20×20=400 (RT/Duroid 5880, $\epsilon_r = 2.33$ )	1.07/(6.95) / (14.86–15.93) 0.95/(4.70) / (19.73–20.67)	(1.87)/82.8 (3.87)/82.8
[24]	40×35=1400 (PTFE, $\epsilon_r = 10.2$ )	4.4/(31.4) / (12–16.4) 1.97/(10.66) / (17.53–19.5)	(4.68)/78.4 (3.65)/82.3
[25]	8.95×7.96 = 71.242 (Rogers RT/Duroid 6010, $\epsilon_r = 10.2$ )	0.576/(4.24) / (13.15–13.72) 0.54/(3.31) / (16.04–16.58)	(3.53)/NR (5.56)/NR
[26]	20×15 = 300 (FR4 Epoxy, $\epsilon_r = 4.4$ )	1.90/(12.4) / (14.3–16.2) 1.50/(8.27) / (17.4–18.9) 0.60/(3) / (19.2–19.8)	(5.90)/80.3 (3.37)/81.9 (3.32)/82.5
[27]	24×17 = 408 (ceramic filled bio-plastic composite, $\epsilon_r = 10$ )	2.38/(18.59) / (11.67–14.05) 1.56/(8.23) / (18.19–19.75)	(3.1)/75.3 (4.13)/86.4
Proposed design	20×20=400 (FR4 Epoxy, $\epsilon_r = 4.4$ )	6.2/(40.8) / (12.4–18.6)	(7.44)/88.4

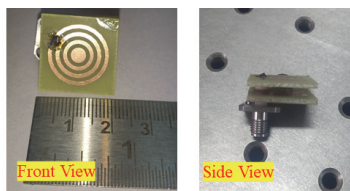
NR=Not Reported, IBW=Impedance Bandwidth

In this work, a novel compact UWB microstrip patch antenna with a defected ground plane is designed for Ku band applications. The antenna is incorporated with multilayer configurations and defected plane for the enhancement of impedance bandwidth. Modeling, simulation, and parametric analysis of the antenna have been performed by the ANSOFT High-Frequency Structure Simulator (HFSS) and the measurement of the proposed structure is carried out by VNA-E5071C.

## II. ANTENNA DESIGNING AND CONFIGURATION

The geometrical configuration and fabricated archetype of the proposed patch antenna are shown in Fig 1. The architecture of the antenna consists of three layers: layer 1, layer 2, and layer 3 of thickness  $h_1$ ,  $h_2$ , and  $h_3$  respectively, stacked to each other (c.f. Fig 1(d)). Layer 1 consists of a conducting patch in the form of circular rings of different radii, printed on an FR4 epoxy substrate as shown in Fig 1(a) and (d). The width of each circular ring is  $r_2$  and the separation between each ring is  $r_1$ . Layer 2 is a dielectric (air) layer of thickness  $h_2$ , while layer 3 is again an FR4 epoxy substrate printed on both sides by conducting copper surface. The lower patch and ground plane is designed on layer 3. A lower patch is incorporated with a slot of dimension  $(L_3 \times W_3)$  mm<sup>2</sup> and it is electromagnetically coupled with the upper patch (c.f. Fig 1(b) & (d)). The bottom view of layer 3 has a defected ground plane of the rectangular shape of size  $L_1 \times W$  mm<sup>2</sup> (c.f. Fig 1(c)). A coaxial SMA connector of a characteristic impedance of 50 Ω is used to excite the proposed patch antenna. The dimensions of the proposed patch antenna with labels are presented in Table 2.





(e)

Fig. 1. Schematic configuration of the proposed patch antenna (a) Top view of layer 1 (upper patch), (b) Top view of layer 3 (lower path), (c) Bottom view of layer 3 (ground plane), (d) side view, (e) Fabricated antenna photographs and measurement setup

TABLE 2  
DIMENSIONAL SPECIFICATION

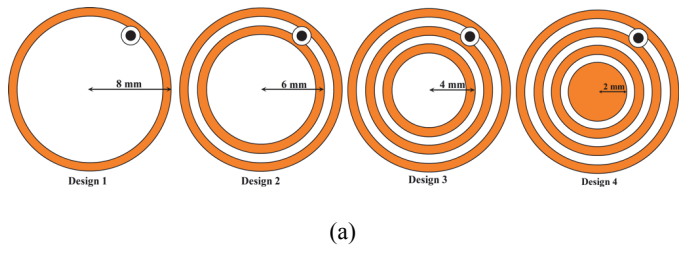
Parameters	Specifications
Substrate materials ( $\epsilon_r$ )	FR4 epoxy (4.4) (for layers 1 & 3), Air (1) (for layer 2)
Thickness of dielectric layers 1, 2 & 3 ( $h_1 = h_2 = h_3$ )	1.6 mm
Dimension of the substrate ( $L \times W$ )	(20 × 20) mm <sup>2</sup>
Dimension of the defected ground plane ( $L_1 \times W$ )	(10 × 20) mm <sup>2</sup>
Dimension of the lower patch ( $L_2 \times W_2$ )	(16 × 10) mm <sup>2</sup>
Dimension of slot on the lower patch ( $L_3 \times W_3$ )	(12 × 2) mm <sup>2</sup>
Ring width ( $r_2$ )	1 mm
Gap between rings ( $r_1$ )	1 mm
Feed location from the center (0, 0) of the patch ( $X_0, Y_0$ )	(3 mm, 6 mm)

### III. RESULTS AND PARAMETRIC ANALYSIS

The antenna results are discussed in terms of return loss (dB), VSWR, gain (dB), radiation efficiency, radiation pattern, and group delay (ns). The parametric study of the proposed patch antenna is also carried out to investigate the effect of various physical parameters such as the dimension of the rectangular slot made on the lower patch and the number of circular rings (N) on the return loss ( $S_{11}$ ) characteristics of the designed antenna. To perform the parametric analysis, change the values of one of the parameters keeping all other parameters constant.

#### A. Variation in the Number of Circular Rings

The proposed optimized circular ring structure is obtained after performing the investigation of the effect of the circular rings made on the top of layer 1. These circular rings work as the radiating elements, named the upper patch elements, as shown in Fig 1(a). Figure 2(a) represents the schematic layout of the upper patch with a different number of rings. Design 1 consists of a circular ring of radius 8 mm, design 2 consists of 2 circular rings with a radius of 6 mm and 8 mm, and design 3 consists of 3 circular rings of radius 8, 6, and 4 mm respectively. Design 4 is obtained from design 3 after introducing the circular patch of radius 2 mm at the center of the antenna structure. The effect of the variation of the number of circular rings on the return loss characteristics is shown in Fig. 2(b). From a perusal of Fig. 2(b), it is clear that design 1 and design 2 antenna configurations have dual wideband behavior while design 3 and design 4 antenna configurations represent single ultra-wideband. The impedance bandwidths of all of the proposed designs are tabulated in Table 3. It is clear from Table 3 that among the proposed designs, design 4 is selected as the final antenna structure because it has the largest impedance bandwidth (6.2 GHz) for ultra-wideband applications in all of the reported structures.



(a)

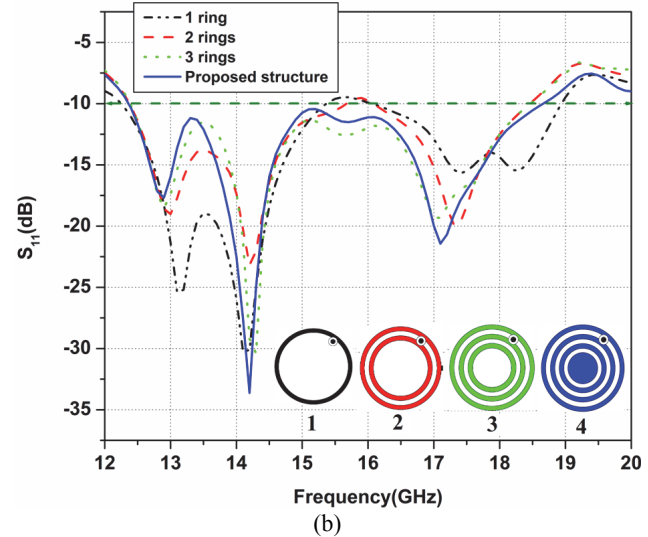


Fig. 2. (a) Layout of the upper patch with a different number of circular rings, (b)  $|S_{11}|$  (dB) variation with respect to the number of circular rings in the antenna structure

TABLE 3  
IMPEDANCE BANDWIDTH OF THE ANTENNA DESIGNS 1, 2, 3, 4

Antenna structures	Bandwidth range / (Impedance bandwidth) (in GHz)
Design 1 (Dual band)	12.3-15.3/(3) & 16.0-18.89/(2.89)
Design 2 (Dual band)	12.4-15.7/(3.3) & 16.10-18.39/(2.29)
Design 3 (Ultra-wideband)	12.4-18.4/(6)
Design 4 (Ultra-wideband) (proposed design)	12.4-18.6/(6.2)

*B. Variation in the Width ( $W_3$ ) of a Rectangular Slot on a Lower Patch*

Figure 3(a) represents how the variation in the rectangular slot dimension affects the performance of the proposed antenna. The parametric analysis in terms of the width ( $W_3$ ) of the rectangular slot made on the lower patch is carried out. From the perusal of Fig 3(a), it can be seen that the antenna behaves like a UWB antenna for  $W_3 = 2$  mm and behave like a dual band antenna for other mentioned values of  $W_3$ . After observing the whole band of spectrum in Fig 3(a), it can be stated that the variation in the slot width does not affect the  $|S_{11}|$  characteristics at the higher range of frequencies (16-18 GHz) in comparison to the lower range of frequencies (12-15 GHz). It is observed that for the lower range of frequency, as the width of the slot is increasing, the lowest cutoff frequency is shifted towards the high frequency, which yields a decrement in the impedance bandwidth. The values of impedance bandwidth for different slot widths are tabulated in Table 4.

TABLE 4  
IMPEDANCE BANDWIDTH RANGE FOR DIFFERENT VALUES OF RECTANGULAR SLOT WIDTH

Slot width ( $W_3$ ) dimensions (in mm)	Bandwidth range/ (Impedance bandwidth) (in GHz)
1 mm (Dual band)	12.5-15.7/ (3.2) & 16.0-18.89/(2.89)
2 mm (Ultra-wideband)	12.4- 18.6/(6.2)
3 mm (Dual band)	12.6-14.8/(2.2) & 15.3-18.89/(3.59)
4 mm (Dual band)	13.0-14.9/(1.9) & 15.69-18.3/(2.61)
5 mm (Dual band)	13.4-14.9/(1.5) & 15.5-19.0/(3.5)

The variation in the  $|S_{11}|$  characteristics of the proposed patch antenna is also incorporated with and without a slot in Fig 3(b). From Fig 3(b), without a slot, the designed antenna will behave like a dual-band antenna with impedance bandwidths of 12.5-14.9 (2.4 GHz) and 16.0-19.3 (3.3 GHz).

The simulated and measured  $|S_{11}|$  plot for the proposed antenna is shown in Fig 3 (c). The disparity between observed and simulated values is attributable to antenna manufacturing losses, substrate behavior differences, fringe capacitance, and mechanical limitations in prototype antenna construction, HFSS algorithm approximations (finite element approaches),

and mathematical assumptions applied in the computation of effective length and effective dielectric constant of the patch.

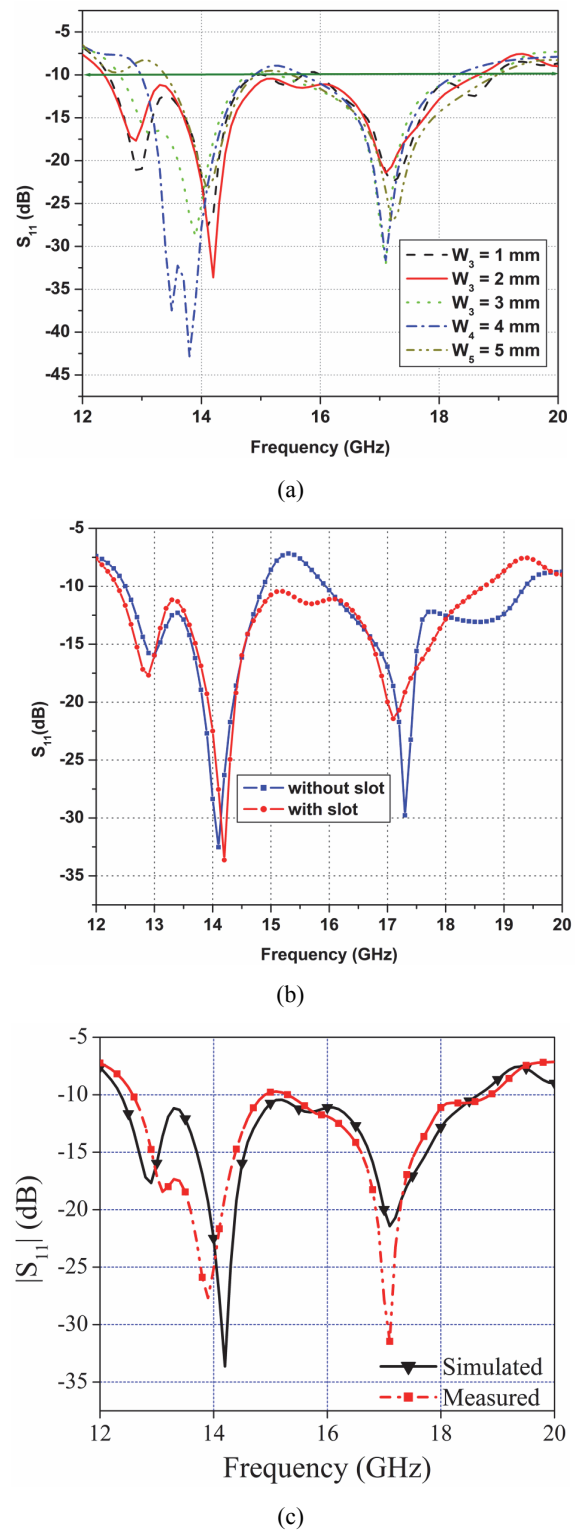
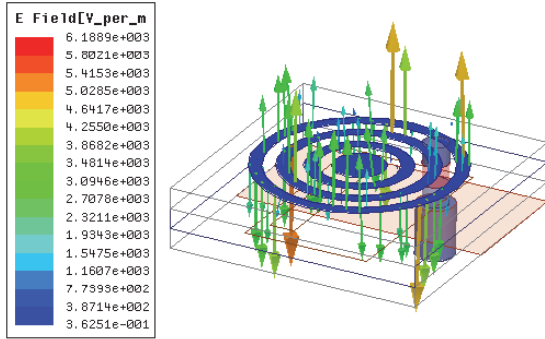


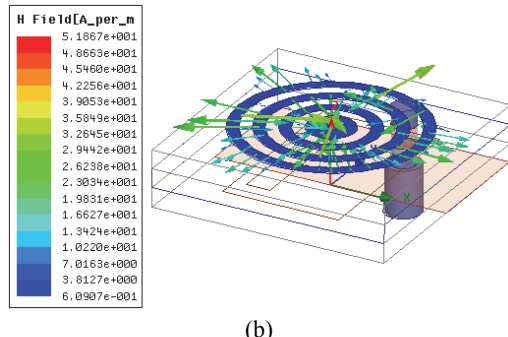
Fig. 3. (a)  $S_{11}$ (dB) variation with frequency for different dimensions of slot width, (b) Variation in  $S_{11}$ (dB) with and without slot for the proposed antenna, (c) Simulated and measured  $|S_{11}|$  of the proposed antenna

### C. Surface Current Distributions and Orientation of Electric and Magnetic Fields of Line

Figures 4(a) & (b) depict the electric field line and magnetic field line orientations on the proposed patch antenna. Figure 4(a) shows that the electric field lines are perpendicular to the 2-dimensional (XY) plane where the radiating patch is stored and are parallel to the z-axis. Figure 4(b) makes it evident that the lines in the magnetic field are perpendicular to the wave's propagation direction and run parallel to the XY plane that is tangential to the radiating patch's surface. As a result of the alignment of the electric and magnetic field lines, the transverse magnetic (TM) mode may be identified as the primary mode of patch propagation.



(a)



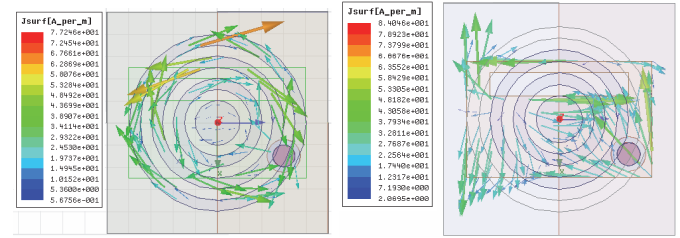
(b)

Fig. 4. (a) Orientation of electric field lines on the proposed patch antenna, (b) Orientation of magnetic field lines on the proposed patch antenna

Figures 5, 6 and 7 represent the simulated surface current distribution of the upper patch, lower patch, and ground plane of the proposed patch antenna at three different resonating frequencies of 12.9 GHz, 14.2 GHz, and 17.1 GHz respectively.

From the perusal of Fig 5, it is observed that when the excitation is provided to the antenna, charge distributions are observed on the upper circular ring patch, lower rectangular slot loaded patch, and conducting ground plane. At the upper patch, most of the surface current is observed at the outermost rings (rings no. 2 and 3 counted from the center) (c.f. Fig 5(a)); at the lower patch, most of the surface current is oriented along the edges of the patch, parallel to the x-axis and at the edge of the slot along the y-axis (c.f. Fig 5(b)); at

the ground plane, most the current is directed outward around the feed (c.f. Fig 5(c)), which make the proposed patch antenna to resonate at 12.9 GHz. The maximum surface current density is observed at 77.42 A/m at the upper patch, 84.04 A/m at the lower patch, and 29.51 A/m at the ground plane.

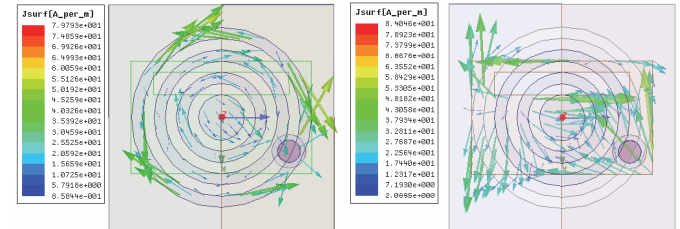


(a)

(b)

(c)

Fig. 5. The surface current distribution of the antenna at 12.9 GHz on (a) Upper patch, (b) Lower patch, (c) Ground plane



(a)

(b)

(c)

Fig. 6. Surface current distribution of the antenna at 14.2 GHz on (a) Upper patch, (b) Lower patch, (c) Ground plane

As shown in Fig 6(a), at the upper circular ring patch, most of the surface current distribution is observed at the outermost ring in a clockwise direction; at the lower patch, most of the current is emitted near the feed and end at the mid of the patch (c.f. Fig 6(b)) while at ground plane most of the current is observed around the feed (c.f. Fig 6(c)). Due to the cumulative

effect of these surface current distributions on the different conducting layers, an antenna has a resonance at 14.2 GHz. At 14.2 GHz, the maximum surface current density is observed 79.79 A/m at the upper patch, 44.22 A/m at a lower patch, and 24.89 A/m at the ground plane.

At the higher resonating frequency of 17.1 GHz, a large surface current distribution is observed at the outermost ring of the upper patch, the circumference of the lower patch and around the feed of the ground plane (cf. Fig 7). The maximum surface current density is observed at 54.68 A/m at the upper patch, 36.84 A/m at the lower patch, and 23.06 A/m at the ground plane.

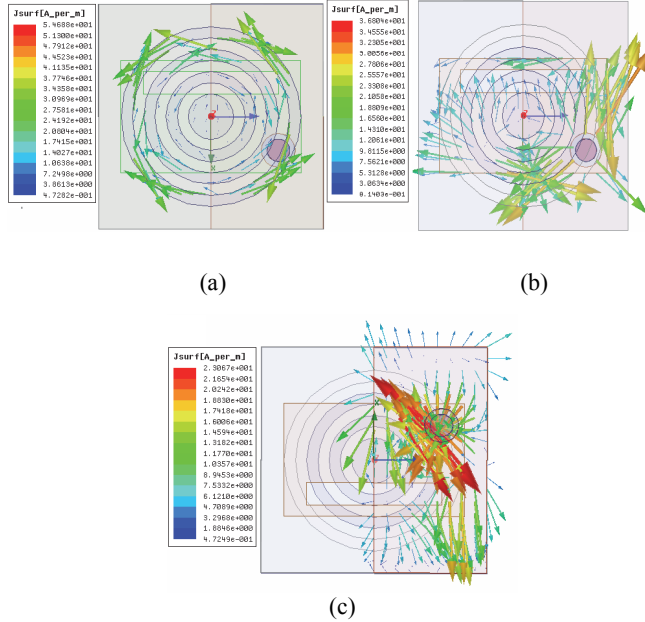


Fig. 7. Surface current distribution of the antenna at 17.1 GHz on  
(a) Upper patch, (b) Lower patch, (c) Ground plane

From the observation of the surface current distributions on different resonating frequencies of 12.9 GHz, 14.2 GHz, and 17.1 GHz, it is clear that the upper conducting circular ring patch has the highest radiation for 12.9 GHz and 17.1 GHz while the lower slot loaded rectangular patch has the highest radiation for 14.2 GHz.

#### D. Gain and Radiation efficiency

Gain (Simulated & Measured) and radiation efficiency plots are shown in Fig 8. Within the operating bandwidth (12.4–18.6 GHz) of the proposed antenna, the maximum value of gain and radiation efficiency is observed at 7.42 dB and 88.40 % while the minimum value is 3.04 dB and 70 % respectively. The simulated and measured gain is found to be in consonance.

Figure 9 represents the variation of the gain and return loss ( $S_{11}$ ) with frequency for the operating bandwidth (12.4–18.6 GHz). To understand the gain variation, the whole impedance bandwidth is divided into three different regions: region 1, region 2, and region 3 (c.f. Fig 9). The occurrence of two or many resonating frequencies in a single operating bandwidth could be termed “ringing resonant frequencies”. The ringing

effect is observed in region 1 (12.53–14.71 GHz). Because of this ringing frequency effect, gain at the first resonating frequency (12.9 GHz) has a higher value compared to the second resonating frequency (14.2 GHz). A decrease in gain is seen at the second ringing resonating frequency, indicating that the ringing phenomena reduce the antenna's gain performance. In region 2(14.83–16.50 GHz), the highest gain is achieved as no ringing effect is observed in this region, while in region 3(16.57–18.43 GHz), again decrement in gain is observed because of the third ringing resonating frequency (17.1 GHz).

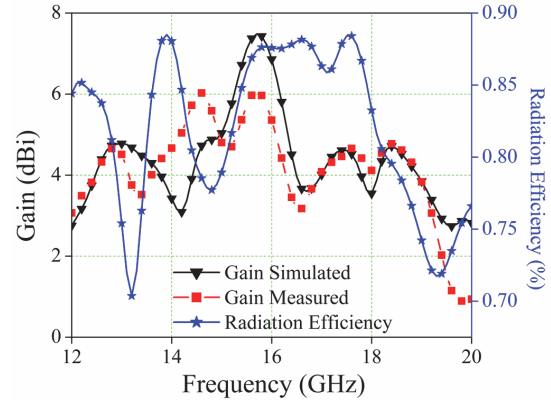


Fig. 8. Gain and radiation efficiency of the proposed antenna

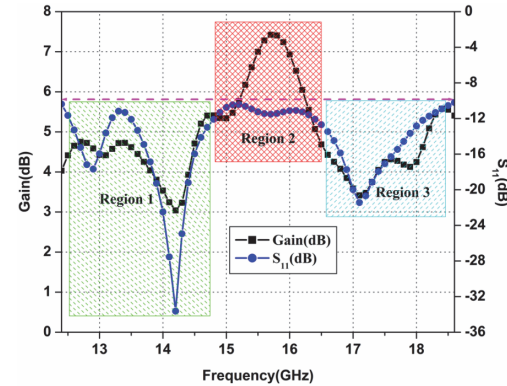


Fig. 9. Variation of gain (dB) and  $S_{11}$  (dB) with respect to frequency for the proposed antenna

#### E. VSWR and Group Delay

Figures 10 and 11 respectively illustrate the patch antenna's VSWR and group delay plots. According to the VSWR plot, it is apparent that the value of VSWR is less than 2 throughout the entire impedance bandwidth range (12.4–18.6 GHz) of the antenna. This indicates that there is a good impedance matching between the excitation port and the proposed antenna within the operating bandwidth range. Group delay pattern is an important factor for the ultra-wideband antenna as it provides information regarding the distortion in the transmitted pulse during communication. The value of group delay should be less than 2 ns for the distortion less transmission of the pulse. From the perusal of Fig 11, it is observed that the value of group delay is less than 1.5 ns for

the proposed patch antenna in the operating bandwidth range from 12.4 GHz to 18.6 GHz.

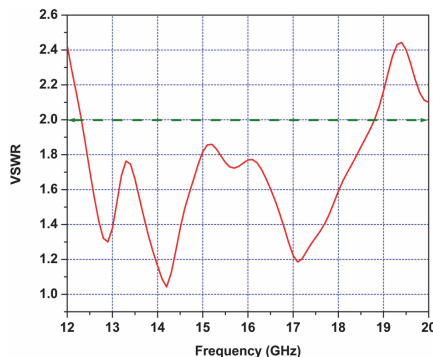


Fig. 10. VSWR of the proposed antenna

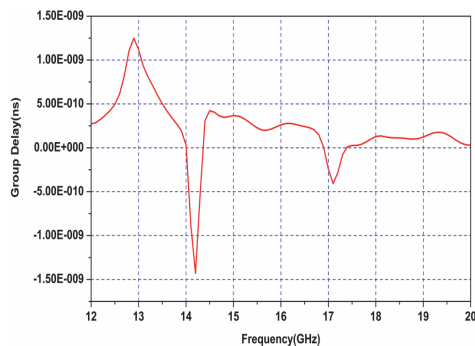


Fig. 11. Group delay of the proposed antenna

### F.3-D Gain Plot and 2-D Radiation Pattern

The 3-dimensional (3-D) gain plots for the proposed patch antenna at three different resonating frequencies of 12.9 GHz, 14.2 GHz, and 17.1 GHz are shown in Fig 12 (a), (b) and (c) respectively.

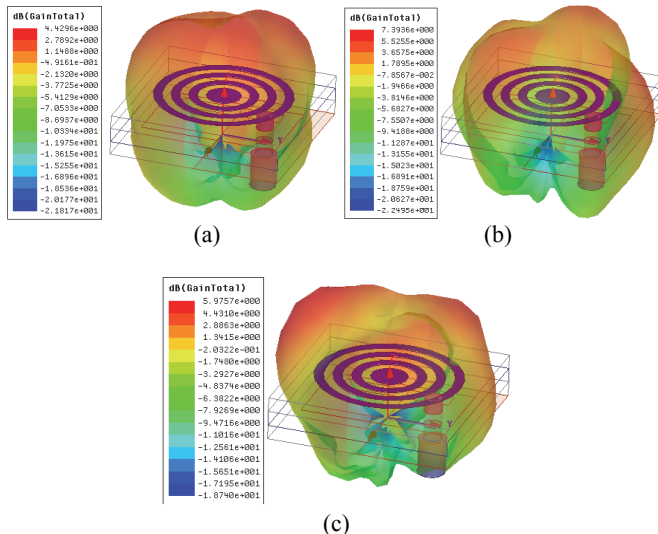
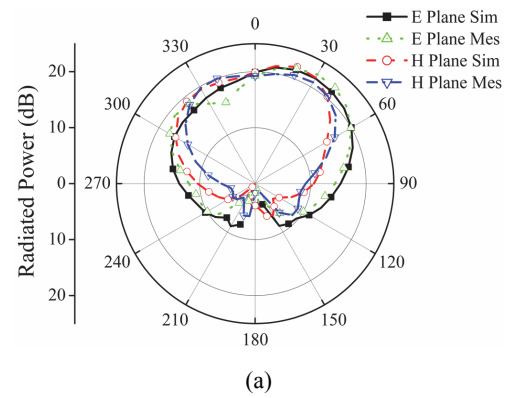


Fig. 12. 3-D gain plot of the proposed patch antenna at, (a) 12.9 GHz, (b) 14.2 GHz, (c) 17.1 GHz

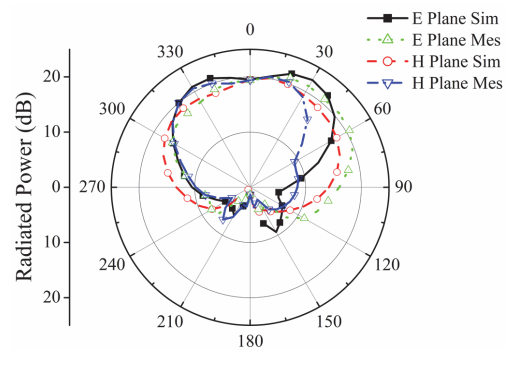
The 3-D plot of the gain provides additional information regarding the distribution of the power radiated from the patch

around the space. From the perusal of Fig 12, it is observed that most of the power is radiated in the upward direction, above the circular ring patch. The value of peak gain at three resonating frequencies of 12.9 GHz, 14.2 GHz, and 17.1 GHz is 4.42 dB, 7.39 dB, and 5.97 dB respectively.

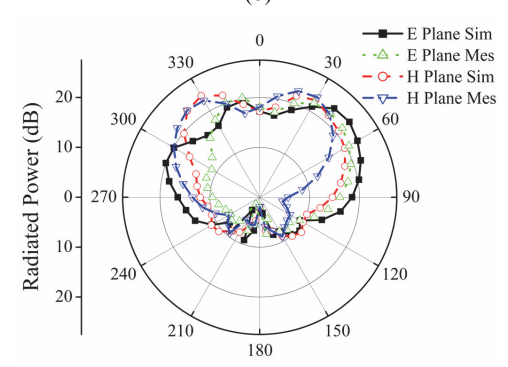
The 2-dimensional (2-D) measured and simulated far-field radiation patterns in the E-plane and H-plane at three different resonating frequencies of 12.9 GHz, 14.2 GHz, and 17.1 GHz are presented in Fig 13 (a), (b) and (c) respectively. From the perusal of Fig 13, it is evident that most of the power is radiated in a broadside direction in both E-plane and H-plane. For the lower frequency (12.9 and 14.2 GHz), the radiation pattern has Omni-directional behavior above the patch while as the frequency increases (17.1 GHz) the radiation pattern represents slightly directional behavior (c.f. Fig 13 (c)).



(a)



(b)



(c)

Fig. 13. 2-D far-field radiation pattern in E-plane and H-plane for the proposed antenna at (a) 12.9 GHz, (b) 14.2 GHz, and (c) 17.1 GHz

#### IV. CONCLUSION

A compact multilayer stacked ultra-wideband (UWB) microstrip patch antenna is presented. The impedance bandwidth of the antenna is reported at 6.2 GHz (12.4 – 18.6 GHz) with a peak gain of 7.42 dB and maximum radiation efficiency of 88.40%, which make the proposed patch antenna a suitable candidate for the Ku band (12-18 GHz) wireless applications. Parametric analysis is carried out in terms of the number of circular rings formed at the upper patch and the width of the rectangular slot made on the lower patch to obtain the optimum antenna configuration for UWB applications. The ringing frequency concept is also discussed in the results from which a conclusion is drawn out that the gain performance of the antenna is degraded because of the ringing effect.

#### REFERENCES

- [1] D. M. Pozar, D. H. Schaubert, *Microstrip Antennas: The Analysis and Design of Microstrip Antennas and Arrays*, New York, Wiley-IEEE Press, 1995.
- [2] B. Mishra, V. Singh, R. K. Singh, N. Singh and R. Singh, “A Compact UWB Patch Antenna with Defected Ground for Ku/K Band Applications”, *Microwave and Optical Technology Letters*, vol. 60, pp. 1–6, 2018.
- [3] B. Mishra, V. Singh and R. Singh, “Dual and Wide-Band Slot Loaded Stacked Microstrip Patch Antenna for WLAN/WiMAX Applications”, *Microsystem Technologies*, vol. 23, pp. 3467–3475, 2017.
- [4] V. Singh, B. Mishra, P. N. Tripathi and R. Singh, “A Compact Quad-Band Microstrip Antenna for S and C-Band Applications”, *Microwave and Optical Technology Letters*, vol. 58, pp. 1365–1369, 2016.
- [5] A. Singh, S. Singh, “A Novel CPW-Fed Wideband Printed Monopole Antenna with DGS”, *AEU - International Journal of Electronics and Communications*, vol. 69, pp. 299–306, 2015.
- [6] P. Khanna, A. Sharma, K. Shinghal and A. Kumar, “A Defected Structure Shaped CPW-Fed Wideband Microstrip Antenna for Wireless Applications”, *Journal of Engineering*, pp. 1–7, 2016.
- [7] A. Nouri, G.R. Dadashzadeh, “A Compact UWB Band-Notched Printed Monopole Antenna with Defected Ground Structure”, *IEEE Antennas and Wireless Propagation Letters*, vol. 10, pp. 1178–1181, 2011.
- [8] A. K. Gautam, A. Bisht and B. K. Kanaujia, “A Wideband Antenna with Defected Ground Plane for WLAN/WiMAX Applications”, *AEU - International Journal of Electronics and Communications*, vol. 70, pp. 354–358, 2016.
- [9] J. Pei, A. G. Wang, S. Gao and W. Leng, “Miniaturized Triple-Band Antenna with a Defected Ground Plane for WLAN/WiMAX Applications”, *IEEE Antennas and Wireless Propagation Letters*, vol 10, pp. 298–301, 2011.
- [10] M. A. Antoniades, G. V. Eleftheriades, “A Compact Multiband Monopole Antenna With a Defected Ground Plane”, *IEEE Antennas and Wireless Propagation Letters*, vol.7, pp. 652–655, 2008.
- [11] Federal Communications Commission Report. n.d. [https://transition.fcc.gov/Bureaus/Engineering\\_Technology/Orders/2002/fcc02048.pdf](https://transition.fcc.gov/Bureaus/Engineering_Technology/Orders/2002/fcc02048.pdf). (accessed October 9, 2019).
- [12] C.-Y.-D. Sim, W.-T. Chung and C.-H. Lee, “Compact Slot Antenna for UWB Applications”, *IEEE Antennas and Wireless Propagation Letters*, vol. 9, pp. 63–66, 2010.
- [13] J. Pourahmazdar, C. Ghobadi, J. Nourinia, N. Felegari and H. Shirzad, “Broadband CPW-Fed Circularly Polarized Square Slot Antenna with Inverted-L Strips for UWB Applications”, *IEEE Antennas and Wireless Propagation Letters*, vol. 10, pp. 369–372, 2011.
- [14] M. Gopikrishna, D. D. Krishna, C. K. Anandan, P. Mohanan and K. Vasudevan, “Design of a Compact Semi-Elliptic Monopole Slot Antenna for UWB Systems”, *IEEE Antennas and Wireless Propagation Letters*, vol. 57, pp. 1834–1837, 2009.
- [15] M. R. Ghaderi, F. Mohajeri, “A Compact Hexagonal Wide-Slot Antenna with Microstrip-Fed Monopole for UWB Application”, *IEEE Antennas and Wireless Propagation Letters*, vol. 10, pp. 682–685, 2011.
- [16] R. Azim, M. T. Islam and N. Misran, “Compact Tapered-Shape Slot Antenna for UWB Applications. *IEEE Antennas and Wireless Propagation Letters*, vol. 10, pp. 1190–1193, 2011.
- [17] M. Sun, Y. P. Zhang and Y. Lu, “Miniaturization of Planar Monopole Antenna for Ultrawideband Radios”, *IEEE Antennas and Wireless Propagation Letters*, vol. 58, pp. 2420–2425, 2010.
- [18] M. H. Ullah, M.T. Islam and J.S. Mandeep, “Printed Prototype of a Wideband S-Shape Microstrip Patch Antenna for Ku/K Band Applications”, *The Applied Computational Electromagnetics Society Journal (ACES)*, vol. 28, pp. 307–313, 2013.
- [19] M. R. Ahsan, M. H. Ullah, F. Mansor, N. Misran and T. Islam, “Analysis of a Compact Wideband Slotted Antenna for Ku Band Applications”, *International Journal of Antennas and Propagation*, 2014.
- [20] C. Yu, W. Hong, Z. Kuai and H. Wang, “Ku-Band Linearly Polarized Omnidirectional Planar Filtenna”, *IEEE Antennas and Wireless Propagation Letters*, vol. 11, pp. 310–313, 2012.
- [21] R. Azim, M. T. Islam and N. Misran, “Dual Polarized Microstrip Patch Antenna for Ku-Band Application”, *Informacije MIDEV*, vol. 41, pp. 114–117, Ljubljana, Slovenia, 2011.
- [22] P. C. Prasad, N. Chattoraj, “Design of Compact Ku Band Microstrip Antenna for Satellite Communication”, *2013 International Conference on Communication and Signal Processing*, pp. 196–200, India, 2013.
- [23] M. M. Islam, M. T. Islam and M. R. I. Faruque, “Dual-Band Operation of a Microstrip Patch Antenna on a Duroid 5870 Substrate for Ku- and K-Bands”, *The Scientific World Journal*, 2013.
- [24] M. R. Ahsan, M. T. Islam, M. H. Ullah, R. W. Aldhaheri and M. M. Sheikh, “A New Design Approach for Dual-Band Patch Antenna Serving Ku/K Band Satellite Communications”, *International Journal of Satellite Communication and Networking*, vol. 34, pp. 759–69, 2016.
- [25] M. Samsuzzaman, M. T. Islam, B. Yatim and M. A. M. Ali, “Dual Frequency Triangular Slotted Microstrip Patch Antenna for Ku Band Applications”, *Przeglad Elektrotechniczny*, vol. 89, pp. 275–279, 2013.
- [26] M. H. Ullah, M. T. Islam, M. R. Ahsan, J. S. Mandeep and N. Misran, “A Dual Band Slotted Patch Antenna on Dielectric Material Substrate”, *International Journal of Antennas and Propagation*, pp. 1–7, 2014.
- [27] M. R. Ahsan, M. T. Islam and M. H. Ullah, “A Simple Design of Planar Microstrip Antenna on Composite Material Substrate for Ku/K Band Satellite Applications”, *International Journal of Communication Systems*, vol. 30, 2017.